Investigation of Solvent Type and Salt Addition in High Transference Number Nonaqueous Polyelectrolyte Solutions for Lithium Ion Batteries

Kyle M. Diederichsen,[†,§] Kara D. Fong,[†,§] Rickey C. Terrell,[†] Kristin A. Persson,[‡,§] and Bryan D. McCloskey*[,†,§]

[†]Department of Chemical and Biomolecular Engineering and [‡]Department of Materials Science and Engineering, University of California, Berkeley, Berkeley, California 94720, United States

[§]Energy Storage and Distributed Resources Division, Lawrence Berkeley National Laboratory, Berkeley, California 94720, United States

S *Supporting Information*

ABSTRACT: High Li$^+$ transference number electrolytes have attracted recent interest as a means to improve the energy density and rate capabilities of current lithium ion batteries. Here the viscosity and transport properties of a sulfonated polysulfone/poly(ethylene glycol) copolymer that displays both high transference number and high conductivity when dissolved in dimethyl sulfoxide (DMSO) are investigated for the first time in a battery-relevant solvent of nearly equivalent dielectric constant: mixed ethylene carbonate (EC)/dimethyl carbonate (DMC). The addition of a binary salt to each solution is investigated as a means to improve conductivity, and the diffusion coefficient of each species is tracked by pulse field gradient nuclear magnetic resonance (PFG-NMR). Through the ^{7}Li NMR peak width and quantum chemistry calculations of the dissociation constant, it is shown that although the two solvent systems have nearly equivalent dielectric constants, the conductivity and transference number of the EC/DMC solutions are significantly lower as a result of poor dissociation of the sulfonate group on the polymer backbone. These results are the first study of polyelectrolyte properties in a battery-relevant solvent and clearly demonstrate the need to consider solvent properties other than the dielectric constant in the design of these electrolytes.
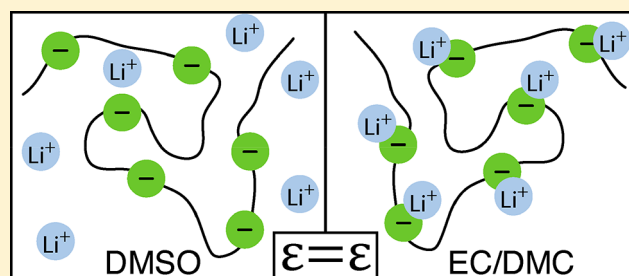
■ INTRODUCTION

Lithium ion batteries are the state-of-the-art energy storage device for portable consumer electronics and electric vehicles. Despite their widespread success, much work remains in further improving cell performance. Of particular interest is the electrolyte, which can limit a battery's energy density and rate capability through numerous issues, including concentration polarization.[1,2] Current state-of-the-art battery electrolytes are composed of a well-dissociated binary lithium salt, such as lithium hexafluorophosphate (LiPF$_6$) or lithium bis(trifluoromethanesulfonyl)imide (LiTFSI), in a blend of ethylene carbonate (EC) and a linear carbonate like dimethyl carbonate (DMC) to provide both high conductivity and favorable electrode passivation toward parasitic side reactions.[3,4] EC, which imparts a stable solid electrolyte interface at the graphite anode, is typically utilized in a mixture due to its slightly above room temperature melting point and high viscosity.[5,6]

The conductivity of these battery electrolytes is on the order 1−10 mS/cm, but the majority of this conductivity is the result of anion motion rather than motion of the electrochemically active Li$^+$. This high anion mobility allows concentration gradients to form within the cell, among other issues. The Li-ion transference number characterizes the fraction of total conductivity arising from lithium motion, being roughly 0.4 in most liquid Li battery electrolytes.[7] Research in high transference number electrolytes (HTNEs), in which the anion is less mobile than the lithium, has focused on ceramic lithium conductors,[8] solid polymer electrolytes,[9] swollen gel polymer electrolytes,[10] and composite electrolytes.[11,12] In most cases there is either a trade-off between conductivity and transference number or the need for a significant re-engineering of the standard Li-ion cell. Recently, the use of nonaqueous polyelectrolyte solutions, where a bulky polyanion is neutralized by lithium ions, has been proposed as a promising route to high transference number, high conductivity electrolytes that would not require a significant redesign of current cell configurations.[13,14]

Thus far, the only studies that have specifically investigated Li ion transport through a nonaqueous polyelectrolyte solution have used dimethyl sulfoxide (DMSO), a highly polar solvent

that can solubilize highly charged macromolecules.[13−15] Unfortunately, DMSO is unsuitable for battery applications due to coinsertion of DMSO with lithium into graphite electrodes, effectively exfoliating the graphite and destroying the electrodes.[16] It is thus important to determine the fundamental design challenges remaining to create an HTNE composed of a lithium neutralized polyanion dissolved in the battery-relevant EC/DMC blend solvent.

Polyelectrolyte solutions have been studied for many years in water due to their utility in understanding the fundamental physics of complex charged biological macromolecules such as proteins and DNA. The reader is referred to the recent perspective of Muthukumar as well as several reviews of polyelectrolyte literature for the larger context of this work.[17−20] A battery electrolyte, however, requires a non-aqueous environment where ion pairing is typically more prevalent than in water, and solvent properties can vary significantly. Polyelectrolytes have been studied in some polar organic solvents, though to our knowledge no study has ever examined a fully dissolved polyelectrolyte in any battery-relevant carbonate solvent. Hara has twice reviewed much of the nonaqueous polyelectrolyte work, though typically the motivation has ultimately been to further understand the polyion behavior in aqueous solution.[21,22]

The motion of polyions and their counterions together has been considered extensively in the literature.[23] However, the goal of much of this work was to interpret the results of experiments such as dynamic light scattering and conductivity measurements to further understand the fundamental physics of the polyion in solution, rather than optimization of any particular transport property.[24] In designing an HTNE, the goal is ultimately to optimize the transport of the lithium counterion through the solution, and thus this design necessitates a re-examination of the classical polyelectrolyte experiments and theories.

The most commonly discussed property of counterions in polyelectrolyte solutions is their effect on charge shielding, which dictates the charge repulsion between ionic groups on the polymer backbone and thus strongly influences polymer conformation.[25−29] In discussing charge interactions in solution, most classical theories of polyelectrolyte conformation rely on the Bjerrum length $l_B = e^2/\varepsilon k T$, where e is the elementary charge, kT is the thermal energy, and ε is the dielectric constant of the solvent. Manning's original theories predict that once the distance between charges on a polymer backbone moves below a certain critical value (the Bjerrum length), ions will begin to condense on the chain to neutralize the charge.[27] Though numerous more recent results and theories have demonstrated the failings of this model for flexible, irregular polymers, the concept of counterion condensation on highly charged polymers to describe the polymer conformation and the dependence of theories on the Bjerrum length are fundamental to the field.[17,30,31] The dielectric constant is therefore typically the first property considered when examining polyelectrolyte data, particularly when using solvents other than water.

As a first step to address the fundamental lack of understanding of polyelectrolytes in battery-relevant solvents, we employ a sulfonated polysulfone/poly(ethylene glycol) copolymer that is fully soluble in both DMSO and a 2:1 (v/v) mixture of EC and DMC. We have previously investigated the conductivity of this class of polymer in the dry state due to the relatively wide array of compositions that could be syntheti-

cally achieved.[32] Here we choose a polymer that is fully soluble in EC/DMC and contains appended sulfonate groups, a common ionic group studied in polyelectrolytes. Both solvents have a dielectric constant near 50, and thus reasonably similar behavior would be expected from the classical theory. Here we characterize the transport properties of the polyelectrolyte with and without added LiTFSI salt. From a fundamental standpoint, added salt is frequently used in the polyelectrolyte literature as a means of varying electrostatic screening in solution and reducing viscosity.[33,34] Here it is also investigated from a performance standpoint as a means to increase polyelectrolyte solution conductivity. Additionally, previous studies have not made clear the trade-off in transference number when adding a small molecule salt alongside the polyelectrolyte. This study will aid in identifying the major questions remaining in the design of an HTNE using polyelectrolyte solutions.

■ METHODS

Materials. Poly(ethylene glycol) (M_n = 1500 Da), anhydrous *N*-methyl-2-pyrrolidone, dimethyl sulfoxide, and toluene were purchased from Sigma-Aldrich and used as received. Sulfonated bis(4-chlorophenyl) sulfone was purchased from Akron Polymer Systems and dried for 2 days under vacuum at 80 °C before use. 2,2-Bis(4-hydroxyphenyl)hexafluoropropane was purchased from Chem Impex Intl. and used as received. Anhydrous ethylene carbonate, dimethyl carbonate, and lithium bis(trifluoromethylsulfonyl)imide were purchased from BASF and used as received.

Polymer Synthesis. The polymer employed in this study is shown in Scheme 1, composed of short poly(ethylene glycol) (M_n =

Scheme 1. Structure of the Charged Polymer Used in This Study
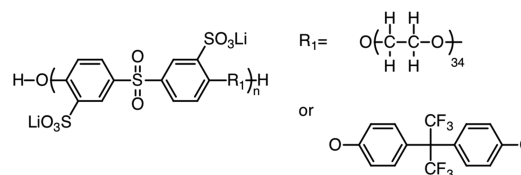
1500 Da) segments with sulfonated sulfone linkages. 10 mol % of a fluorinated biphenol monomer is also incorporated as a tag to track the diffusion of the polymer backbone in a nondeuterated solvent. The polymer was synthesized according to the procedures outlined in ref 32. Briefly, the condensation reaction is performed by loading the three monomers to a reaction vessel with *N*-methyl-2-pyrrolidone and potassium carbonate and allowed to react for 48 h at 190 °C following azeotropic removal of water with toluene for several hours. The polymer is then precipitated in isopropanol, followed by dialysis in water with lithium carbonate to exchange the appended ion to lithium and remove residual solvent and other impurities. The final structure of the polymer was confirmed through NMR; the final ion content of the polymer was verified by inductively coupled plasma optical emission spectroscopy (ICP-OES), and no other trace metallic impurities were observed. The polymer was dried for 2 days at 70 °C over phosphorus pentoxide before use.

Solution Preparation. Each solution was prepared in an argon glovebox (Vacuum Atmospheres) kept below 1 ppm water and oxygen. Polymer solutions were prepared and then added to weighed amounts of LiTFSI salt. No precipitation or aggregation was observed in any solutions over the course of six months. The final lithium concentration of each sample was measured by quantification with ^{7}Li NMR. Standard solutions of LiBr in D_2O were prepared, and a [7]Li spectrum was obtained for each using a consistent receiver gain, calibrated pulse length, and 120 s delay time. A calibration curve was then made. For each solution, the NMR spectra were shimmed on the

^{1}H signal, and then a ^{7}Li spectrum at the same receiver gain was obtained, enabling accurate measurement of the lithium content of each sample. The reported amount of LiTFSI added in each plot in this work is calculated from this measurement.

Conductivity. To minimize the amount of solution necessary for conductivity measurement, the conductivity of each solution was measured using coin cells constructed in the argon glovebox. Each cell was constructed with two stainless steel blocking electrodes and a quartz fiber (Whatman) separator that had been washed and dried prior to use. The coin cells were loaded to a temperature-controlled oven, and the temperature was maintained at 25 °C throughout the measurement. AC impedance was performed on each cell, and the conductivity was determined from the minimum of the phase angle of the resulting spectra. Each value represents the average of at least four cells. The coin cell measurement was calibrated to LiTFSI in DMSO solutions measured both by the same coin cell technique and with a conductivity probe inside of the glovebox.

Viscosity. Viscosity was measured using an electromagnetically spinning viscometer (EMS-1000, Kyoto Instruments). Achieving high accuracy measurements in low volume solutions, this technique measures viscosity based on the rotation rate and magnetically applied force to a 2 mm aluminum ball located in the testing solution. The viscometer was calibrated using known standards (Cannon Instruments Inc.) and was within 3% of the known values. 300 μL of each solution was sealed in the 13 mm diameter test tubes in the argon glovebox. At no point during the measurement, or during sample preparation, were any of the solutions exposed to ambient atmosphere, ensuring that H_2O or other atmospheric contamination was eliminated. Temperature is maintained at 25 °C throughout the measurement, and the reported values represent the average of at least eight individual viscosity measurements on the same solution. Variability in these repeat measurements was also around 3%.

Pulse Field Gradient NMR. Diffusion coefficients of each species were measured by pulse field gradient NMR on a Bruker Avance III 600 MHz instrument fitted with a 5 mm Z-gradient broadband probe and variable temperature unit maintained at 25 °C throughout the measurement. Samples were prepared in the glovebox and capped with an air-free cap and parafilm. The gradient was calibrated to known values of H_2O, H_2O in D_2O,[35] H-DMSO in d_6-DMSO,[36] dimethyl carbonate,[37] and 0.25 and 4 M LiCl in H_2O.[35] The T_1 of each peak monitored was measured, and a recycle delay at least 4 times T_1 was utilized. For ^{7}Li, ^{19}F of TFSI$^-$, and the solvent, a double stimulated bipolar gradient pulse sequence (Bruker's dstebpgp3s program) was used.[38] Because of the low signal and slow diffusion of the polymer backbone, the longitudinal eddy delay program without convection compensation (Bruker's ledbpgp2s program) was employed to monitor the diffusion of the ^{19}F peak associated with the polymer backbone.[39] The diffusion of this peak was confirmed to match the diffusion of the proton polymer peaks via a separate measurement in d_6-DMSO where the polymer ^{1}H peaks are not impacted by the solvent signal. For the dstebpgp3s program, the signal intensity as a function of gradient strength was fit to

$$\frac{I}{I_0} = e^{-\gamma^2 g^2 \delta^2 D(\Delta - 5\delta/8 - \tau)} \tag{1}$$

where γ is the gyromagnetic ratio, g is the gradient strength, δ is the duration of the gradient pulse, D is the diffusion coefficient, Δ is the diffusion delay time, and τ is the delay for gradient recovery. The correction for sine-shaped gradient pulses was included here.[40] For the ledbpgp2s program, the equation was modified to

$$\frac{I}{I_0} = e^{-\gamma^2 g^2 \delta^2 D(\Delta - 5\delta/16 - \tau/2)} \tag{2}$$

Diffusion delays employed were between 0.05 and 0.25 s, and gradient pulse lengths were between 0.8 and 5.5 ms. Repeat experiments with varied diffusion delay and pulse length verified the measured diffusion coefficient was independent of experimental condition. Between 8 and 16 experiments with varying gradient strength were used for each diffusion coefficient measurement. Example Stejskal−Tanner plots are

included in the Supporting Information, Figure S1; in all cases a linear decay in signal strength on the Stejskal−Tanner plot was observed. Variability within the gradient calibration was used to estimate a minimum error of 5% on the diffusion coefficients. For some samples the fitting error due to low signal strength was larger than this 5% error. Because of the length of repeated experiments, the maximum of the fitting error and 5% were used to determine error bars for the diffusion measurements.

Calculation of Dissociation Constant. Quantum chemistry calculations were performed with the Gaussian 16 software package[41] using the ωB98X-D functional[42] and the 6-311++G** basis set.[43−45] All calculations consisted of a structure optimization followed by a frequency calculation. The frequency calculations were used to determine thermodynamic properties and verify that no negative frequencies existed. Implicit solvent was incorporated into all of the calculations using the polarizable continuum model (PCM) with the integral equation formalism (IEFPCM).[46−49] Dielectric constants of 46.7 and 51.0 were used for DMSO[50] and EC/DMC,[51] respectively.

Dissociation energies were calculated from the computed Gibbs free energies of the cation (Li$^+$), the anion (based on the anionic moiety of the polymer, see Scheme 2), and the ion pair (cation and

Scheme 2. Structure of the Anionic Moiety Used for Dissociation Energy Calculations^a
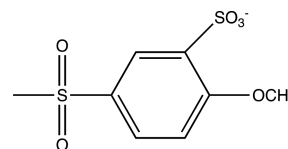
^{a}This structure is essentially the small molecule equivalent of the charged polymer anion moiety shown in Scheme 1 and was used instead of full polymer chains due to the computational cost of large-scale quantum chemistry calculations.

anion together). The difference between the Gibbs free energies (ΔG) of the paired and dissociated states yield the dissociation energy,[52] from which we can obtain the dissociation constant, K ($\Delta G = -RT \ln K$). Thermal contributions to the Gibbs free energy were calculated at 25 °C.

In the explicit solvent calculations, the number of solvent molecules included was chosen to match the Li$^+$ coordination numbers found in previous work. In DMSO, four solvent molecules per Li$^+$ were used based on X-ray and neutron diffraction as well as molecular dynamics studies.[53,54] For the EC/DMC calculations, one DMC and three EC molecules were included per Li$^+$ based on quantum chemistry studies from Borodin et al. showing this solvation shell composition to be most energetically stable among all EC$_n$DMC$_m$/Li$^+$ ($n + m = 4$) complexes.[55] This EC/DMC ratio is approximately equivalent to the bulk molar ratio of the 2:1 (v/v) EC/DMC blend utilized in this work. To determine the sensitivity of the calculated trends to these choices in solvation shell structure, we also computed the dissociation constants for ion pairs with <4 explicit solvent molecules and found that the trend in dissociation energy between DMSO and EC/DMC is consistent for systems with >2 explicit solvent molecules. Initial solvation shell geometries were obtained using a Monte Carlo-based conformational search with MacroModel and the Maestro graphical interface (Schrödinger).[56] The mixed torsional/low-mode sampling method was used in conjunction with the OPLS_2005 force field. The minimum-energy conformer from this analysis was used as the starting geometry for the quantum chemistry calculations.

■ RESULTS AND DISCUSSION

Conductivity is the primary electrolyte property considered when designing a battery electrolyte. Figure 1 displays the conductivity of the polyion with added salt solutions using DMSO (Figure 1A) or EC/DMC (Figure 1B) as the solvent, plotted against the amount of LiTFSI added to the solution.
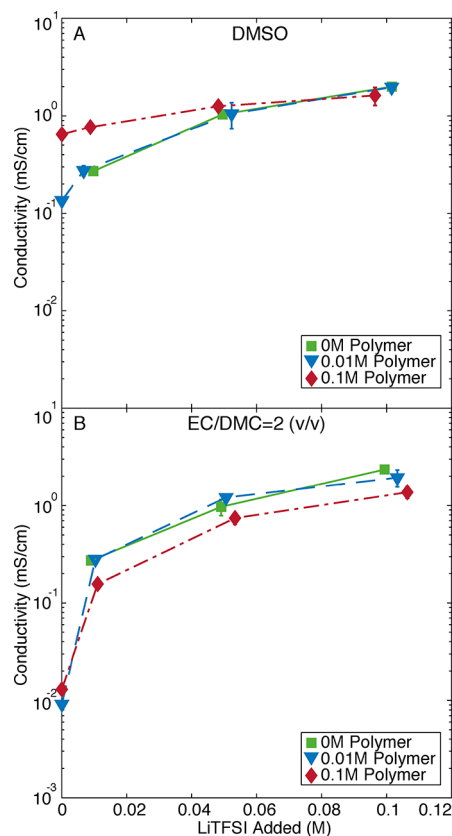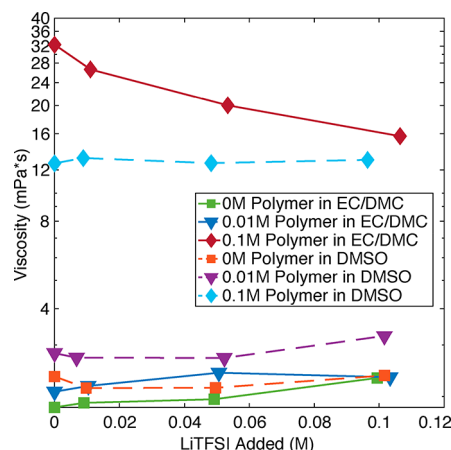
Figure 1. Conductivity as a function of LiTFSI added at each polymer concentration in (A) DMSO and (B) EC/DMC = 2 (v/v).

The polymer molarity reported in all figures corresponds to the appended sulfonate ion molarity in each solution and is therefore twice the molarity of the sulfonated sulfone repeat unit (given that each sulfone repeat unit has two sulfonate groups). This does not, however, correspond directly to the total monomer concentration due to the additional PEG repeat units present. Without polymer (green squares in Figure 1), the plotted LiTFSI concentration corresponds to the total lithium concentration in solution, but for the polymer solutions the total lithium content is the LiTFSI added plus the reported polymer molarity. The conductivity of the pure solvent, which was below 3 μS/cm, was subtracted in each case. It should be noted in all cases here the conductivity of the polymer solutions is several orders of magnitude higher than the neat polymer in the dry state.[32] In both solvents, the conductivity of each solution increases into the range of an acceptable battery electrolyte with addition of LiTFSI, and at 0.01 M polymer, the conductivity of the solution is no different from the solution without polymer at these polymer/LiTFSI concentrations.

At high polymer concentration, the conductivity behavior of solutions made from different solvents deviate. In EC/DMC, the solutions with 0.1 M polymer have a lower conductivity than the solutions with no polymer at each LiTFSI concentration, even though the total lithium concentration of the polymer containing solutions is always higher. This implies that the Li$^+$−SO$_3^-$ pairs appended to the polymer backbone remain substantially, if not completely, associated in EC/DMC and hence do not contribute to conductivity. Therefore, the lower conductivity of the 0.1 M polymer solutions compared to the 0 M polymer solutions results from the higher viscosity

imparted by the addition of polymer to the solution (see Figure 2). In contrast, the polyion and its lithium counterion
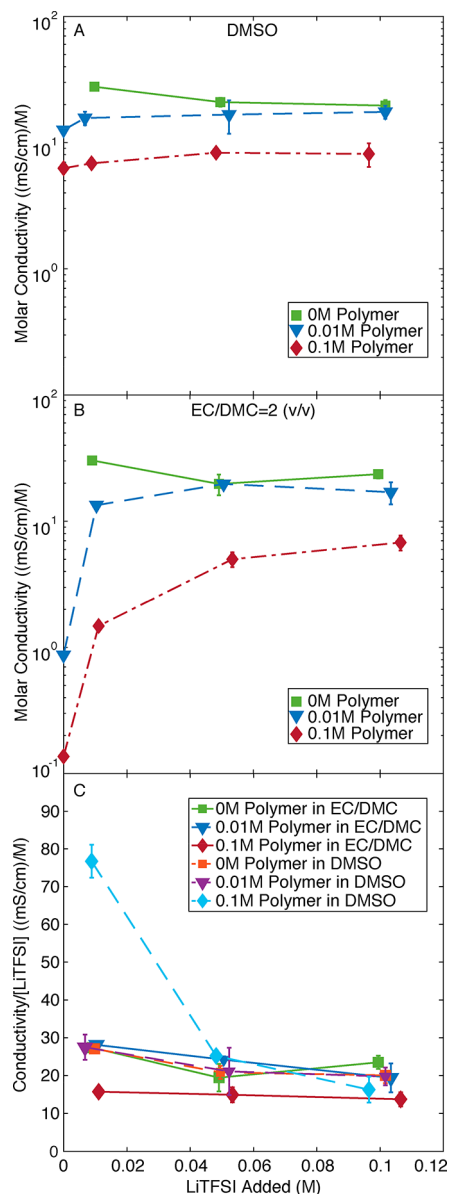

Figure 2. Viscosity as a function of LiTFSI added to each polymer solution for EC/DMC (solid lines) and DMSO (dashed lines). Polymer-free solution data are shown as squares, 0.01 M polymer solution data are represented as triangles, and 0.1 M polymer solution data are represented as diamonds. The 3% error estimated from the calibration is smaller than the data points in this figure.

appear to contribute to the total solution conductivity in DMSO solutions. This is particularly clear at low LiTFSI concentration, where the conductivity is significantly higher for the 0.1 M polyion solutions compared to the 0 M polymer solutions. The increase in conductivity on addition of more LiTFSI is less pronounced in the higher polymer concentration samples, and eventually the conductivity of the 0.1 M polyion solution is equivalent to the conductivity of pure LiTFSI solutions, again despite the significantly higher total lithium concentration.

The viscosity of each solution in Figure 1 is plotted in Figure 2 as a function of the amount of LiTFSI added. In each solvent (dashed vs solid lines), increasing polymer concentration corresponds to an increase in viscosity as would be expected. Without polymer (squares) and with 0.01 M polymer (triangles), only a slight increase in viscosity is noted with addition of LiTFSI, as the concentration of salt is relatively low. At high polymer concentration in DMSO, addition of salt causes no change in viscosity; however, in EC/DMC there is a significant decrease in viscosity with increasing salt concentration. Based on the conductivity of these solutions, these results are generally unexpected. For a charged polymer in solution, addition of small molecule salt is known to cause a decrease in the solution viscosity as a result of charge screening that allows the chain to relax into a smaller conformation.[34] Thus, we would expect that addition of salt to the polymer solutions in DMSO should cause a decrease in the solution viscosity because here the polymer contributes to the total conductivity and so must be charged. In EC/DMC, the polymer does not appear to contribute significantly to the conductivity, indicating it is not charged and that charge screening is unlikely to play a role in the viscosity.

To further investigate these surprising results, we turn first to the molar conductivity in Figure 3A for DMSO and Figure 3B for EC/DMC to more clearly ascertain the polymer contribution to the total conductivity. Here the conductivity is normalized to the total lithium concentration of each solution

Figure 3. Molar conductivity (normalized using total Li$^+$ concentration in each solution) as a function of LiTFSI added at each polymer concentration in (A) DMSO and (B) EC/DMC = 2 (v/v). (C) Conductivity normalized to LiTFSI concentration for all solutions.

and plotted again against the amount of LiTFSI added. In both cases, the pure LiTFSI solution molar conductivity displays negligible concentration dependence, consistent with LiTFSI being a strong electrolyte (nearly fully dissociated). In DMSO, Figure 3A, the polymer solutions display only a slight increase in molar conductivity with added small molecule salt. The effect of viscosity can clearly be seen here in the decreased molar conductivity with increasing polymer concentration. In Figure 3B, where EC/DMC solutions are presented, the polymer solutions display dramatically different behavior than DMSO solutions, with the 0.1 M solution deviating the most from the pure LiTFSI case and showing an increase in molar conductivity as the concentration increases. This would be consistent with the decrease in viscosity with higher salt concentration but could also be explained if the polyion and its counterion did not contribute to the conductivity.

To examine the relative contribution of LiTFSI and polyion to the conductivity, in Figure 3C, the conductivity has been normalized to the concentration of LiTFSI rather than the total lithium concentration. Here, the molar conductivity of the pure LiTFSI and 0.01 M polyion in both EC/DMC and DMSO solutions collapses to a single line that is concentration independent. At 0.1 M polyion, the solution at 0.01 M LiTFSI in DMSO displays dramatically higher molar conductivity, clearly indicating the polyion contributes significantly to the observed conductivity. As the concentration of salt increases, however, the [LiTFSI]-normalized conductivity falls back to similar values as the other solutions. In EC/DMC, the 0.1 M polyion solution conductivity displays no concentration dependence, indicating the large increase with added LiTFSI observed in the Li$^+$-normalized molar conductivity (Figure 3B) can be explained entirely by the addition of LiTFSI and not the decreasing viscosity shown in Figure 2. In this plot, increasing molar conductivity with LiTFSI concentration would be expected if the effect was a result of viscosity. Thus, the conductivity data clearly suggest that the polyion is charged in DMSO and uncharged in EC/DMC, despite the trends in viscosity. It is therefore necessary to further deconvolute each species contribution to these bulk properties.

To do so, the diffusion coefficients from PFG NMR of the polymer backbone, TFSI$^-$ anion, and Li$^+$ counterion are plotted in Figures 4A and 4B for DMSO and EC/DMC, respectively. In both solvents, the diffusion of the TFSI$^-$ anion is independent of salt concentration, is higher than either other species, and appears to slightly decrease at the highest polymer concentration. This decrease in diffusion coefficient at high polymer concentration is observed for all species as a result of the increased viscosity at higher polymer concentration (Figure
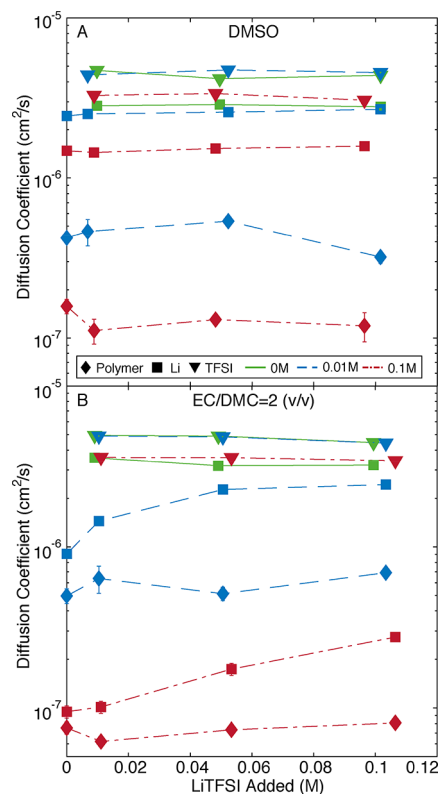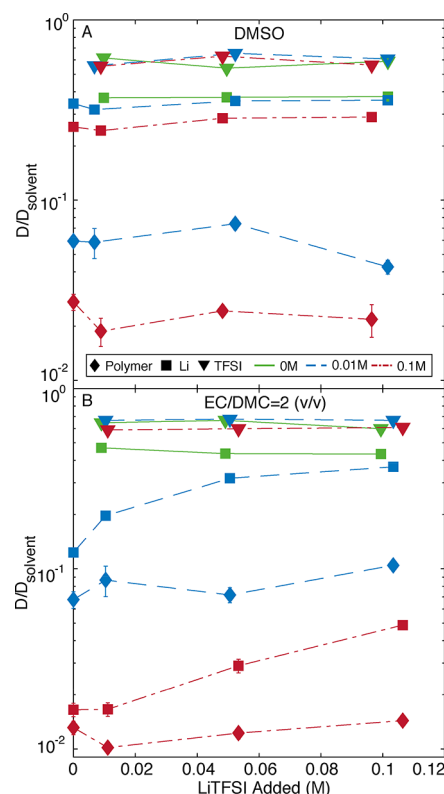

Figure 4. Diffusion coefficients of each species as a function of LiTFSI added for (A) DMSO and (B) EC/DMC = 2 (v/v).

2). The relatively higher diffusion coefficient of TFSI⁻ compared with Li⁺ is expected given the large solvation structure of Li⁺ in solution.[57] The polyion backbone diffusion coefficient also does not appear to have a significant dependence on LiTFSI concentration though is significantly slower at 0.1 M polyion than 0.01 M. This indicates the 0.1 M polyion solution has passed the entanglement concentration, as polyelectrolyte diffusion coefficients are independent of polymer concentration within the semidilute range.[29] It is surprising that the backbone diffusion coefficient is not a function of total LiTFSI concentration in either solution, particularly in EC/DMC where a significant decrease in bulk viscosity is observed at high polymer concentration. The expansion or contraction of chain conformations that might be expected to cause this decrease in viscosity would typically be expected to also affect the diffusion of the chain.

The diffusion coefficient of the lithium is the most drastically different transport property between the two solvents, being independent of LiTFSI concentration in DMSO, but significantly increasing with LiTFSI concentration in EC/DMC. This behavior is consistent with the analysis of the molar conductivity data in EC/DMC which clearly indicates the dissociation of lithium from the polymer is very low. The lithium diffusion reported here is an average of all lithium species in solution, so addition of a fast lithium species (in the form of LiTFSI) to a solution where lithium is tightly associated with a bulky polymer would produce a slowly increasing average. Unfortunately, these different lithium species cannot be directly observed in the diffusion measurement. Given the increase in lithium diffusion with added LiTFSI in EC/DMC, it is somewhat surprising that the average lithium diffusion does not change at all on addition of LiTFSI to the DMSO-based polymer solution. There are two possible explanations for this observation in DMSO. First, the addition of a fast lithium species from LiTFSI could be perfectly balanced by the association of an equivalent amount of lithium to the polymer (producing a slow lithium species). If these processes occur simultaneously, no change in the average Li diffusion would be seen. Such a balance might be reasonable given a dynamic equilibrium between bound and free lithium, where addition of free lithium would drive the balance back to the associated species. Similar suggestions have been made in the literature.[31,58,59] A second possible explanation is that the lithium species present in the pure polymer system diffuses at the same rate as lithium in a pure LiTFSI solution, and at these concentrations the additional ionic content does not produce any change in the species' motion. It can easily be seen from Figure 4A that the lithium in a 0.01 M polyion solution diffuses at nearly the same rate as a lithium species in a pure LiTFSI solution, though at 0.1 M polymer the lithium diffuses somewhat slower.

To examine the local effects of viscosity on the solution directly, we examine the diffusion coefficients relative to the solvent diffusion coefficients in Figure 5. The solvent diffusion coefficients are plotted alone in Figures S2 and S3. Figure 5 plots the diffusion coefficient of each species normalized to the diffusion coefficient of DMSO in Figure 5A and molar average solvent diffusion for EC/DMC in Figure 5B. In each case, the solvent diffusion coefficient, $D_{solvent}$, is that measured for each unique composition reported in Figure 4 from the ¹H spectra. In both solvents, it is immediately evident that any difference in TFSI⁻ diffusion can be ascribed to the slightly slower solvent diffusion in the more viscous 0.1 M polymer solutions,


Figure 5. Diffusion coefficient of each species normalized to the solvent diffusion coefficient as a function of LiTFSI added for (A) DMSO and (B) EC/DMC = 2 (v/v).

as $D/D_{solvent}$ for TFSI⁻ collapse onto a single curve for all polymer and LiTFSI concentrations. TFSI⁻ also appears to diffuse at the same rate in both solvents relative to the solvent diffusion. In EC/DMC, Figure 5B, the normalized lithium diffusion coefficients are significantly lower for the polymer solutions compared to the pure LiTFSI (0 M polymer) solutions, further supporting the conclusion of poor dissociation in EC/DMC. In DMSO, Figure 5A, the normalized lithium diffusion coefficient is closer to the diffusion of lithium in the pure LiTFSI solution but does not collapse completely to a single line. Thus, it is clear that a portion of the lithium must still be associated with the polymer at 0.1 M polymer in DMSO, where $D_{Li}/D_{solvent}$ is still lower at all LiTFSI concentrations than $D_{Li}/D_{solvent}$ for the 0 and 0.01 M polymer cases.

Most surprisingly, the large decrease in viscosity as a function salt concentration in the 0.1 M polymer in EC/DMC series is not accounted for by the diffusion coefficient of the solvent, which remains relatively constant with added salt (Figure S3). While at a given salt concentration there is a decrease in solvent diffusion with increasing polymer concentration that accounts for the change in TFSI⁻ diffusion, there is no significant increase in solvent diffusion coefficient as a function of salt concentration. In fact, at this polymer concentration, the solvent diffusion coefficients appear to decrease slightly with salt concentration.

This deviation from the expected viscosity, η_{Stokes}, based on the observed solvent diffusion coefficients and assuming the molecules diffuse as Stokes spheres, can be observed most directly in Figure 6A,B. The viscosity ratio defined in eq 3 is plotted as a function of salt concentration.
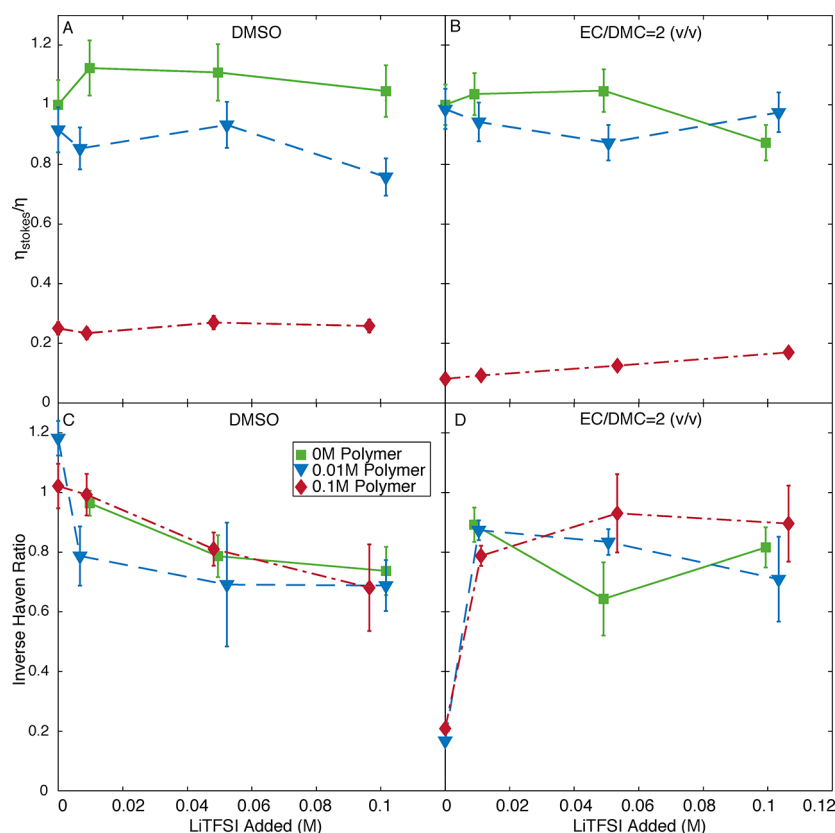
Figure 6. Viscosity ratio defined in eq 3 as a function of LiTFSI added for each polymer concentration in (A) DMSO and (B) EC/DMC = 2 (v/v). Inverse Haven ratio as a function of LiTFSI added for each polymer concentration in (C) DMSO and (D) EC/DMC = 2 (v/v). In each figure, the reported error has been propagated from the measurements.

$$\frac{\eta_{\text{Stokes}}}{\eta} = \frac{kT}{6\pi r_{\text{solvent}} D_{\text{solvent}} \eta} \qquad (3)$$

Here r_{solvent}, the effective hydrodynamic radius of a diffusing solvent molecule, is calculated using the Stokes−Einstein equation, the measured viscosity, and PFG NMR diffusion coefficient of the pure solvent (i.e., without added salt or polymer). For EC/DMC, the diffusion coefficient of the two solvents was averaged on a molar basis to obtain an effective average solvent radius. Deviations from 1 in this ratio could therefore be a result of changes in the effective solvent radius as the solution composition changes or other intermolecular interactions. The most apparent trend here is that the deviation from the "ideal" Stokes viscosity increases with polymer concentration. This suggests that the bulk viscous effects are decoupled from the local viscosity of the solutions. Such phenomena have been discussed in polymer solutions for some time, where it is understood that the length scale of the polymer entanglements that cause high viscosity is longer than would be felt directly by a small probe molecule.[60] Essentially, the small molecule can move around the polymer, but when a bulk shear is applied to the solution, the long chains impede this motion. This suggests that the effect that causes the decrease in viscosity at 0.1 M polymer in EC/DMC occurs over a relatively long range or that the local interaction has a stronger influence on bulk properties than local motion of small ions. This observation is important for the design of an HTNE, where the bulk viscosity might otherwise be considered a key property to minimize.

To relate local diffusion and bulk conductivity measurements directly, the inverse Haven ratio, H_R^{-1}, as defined in eq 4, is often employed.[61]

$$H_R^{-1} = \frac{\sigma}{\frac{F^2}{RT}(c_{\text{Li}}D_{\text{Li}} + c_{\text{sulfonates}}D_{\text{polymer}} + c_{\text{TFSI}}D_{\text{TFSI}})} \qquad (4)$$

F is Faraday's constant, R is the gas constant, and T is the temperature (298 K). Note that c_{Li} is the total lithium concentration, while the two anionic species can be treated separately. Here the measured conductivity (σ) is related to the conductivity that would be expected from the Nernst−Einstein equation if every NMR-measured diffusion coefficient ideally represented all charged species in solution. As this would only be explicitly true if every species was fully dissociated, the Haven ratio is often used to probe extent of dissociation. It should be noted that because the NMR averages all lithium species (charged, uncharged, associated, or dissociated) H_R^{-1} does not directly correspond to extent of dissociation; however, it does relate to the ideality of the solution and the relationship between diffusivity and mobility.[62] In DMSO, Figure 6C, the ratio for the pure 0.1 M polymer solution and most dilute pure LiTFSI solution is equivalent to one, within error of the measurements. The solution at 0.01 M polymer appears to have an $H_R^{-1} > 1$ in the pure solution, a result that was verified twice in this study (two separate multiple-replicate analyses), perhaps alluding to the complex relationship between diffusion and mobility in polyelectrolyte solutions.[63] Detailed analysis of this result is beyond the scope of this paper but should be the subject of future work. As the LiTFSI concentration is increased, H_R^{-1}
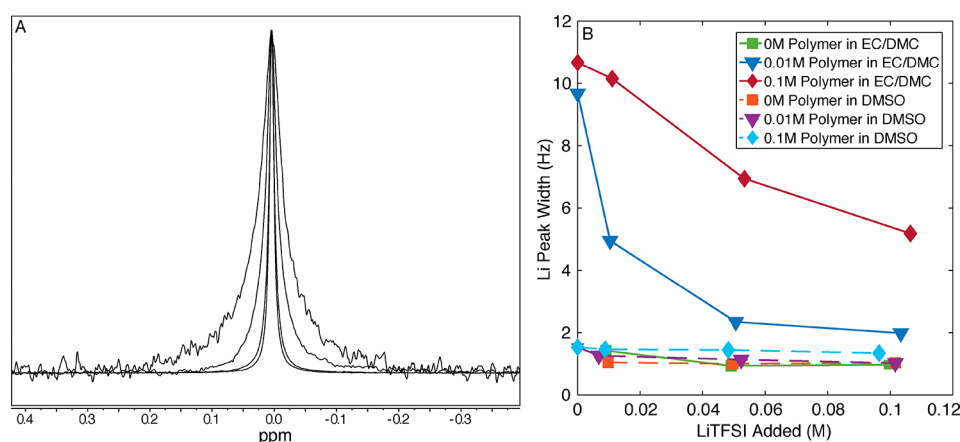
Figure 7. (A) ^{7}Li spectra for the series of solutions at 0.01 M polymer in EC/DMC with added LiTFSI. The spectra of each solution have been overlaid, and the intensity was normalized. With added LiTFSI, the peak width narrows. (B) ^{7}Li peak width at half-maximum as a function of LiTFSI added for all solutions.

decreases, indicating the solution conductivity deviates from the conductivity that would be expected if each NMR-measured diffusion coefficient ideally translated to conductivity. Here this decrease in each solution is likely the result of ion association as concentration is increased. In EC/DMC (Figure 6B), H_R^{-1} of the pure polyelectrolyte solutions is very low, as would be expected for low dissociation. Interestingly, even a small amount of salt causes the Haven ratio to immediately jump to the value for pure LiTFSI. This is a result of the orders of magnitude larger diffusion coefficient of TFSI$^-$ compared to the polyanion combined with the immediate increase in average lithium diffusion coefficient on addition of LiTFSI due to the increased dissociation of LiTFSI compared to the lithium sulfonate moieties on the polymer chain.

It is important to recognize the behavior reported here for the same polymer in DMSO and EC/DMC is surprising. The vast majority of literature on polyelectrolyte solutions uses the dielectric constant of the solvent as the main parameter to determine the charge of the polymer via the Bjerrum length. The dielectric constant of DMSO at 298 K is 46.7, and a 2:1 v/v mixture of EC and DMC should have a dielectric constant at least equivalent to or higher than DMSO.[50] It should be noted that a carefully measured value for EC/DMC could not be found at 298 K but has been carefully measured at 313 K to be 51.[51] The dielectric constant of a blend of EC and ethyl methyl carbonate at an equivalent ratio is also near 50.[64] On the basis of this alone, it would be expected that the two polyelectrolyte solutions have similar ion dissociations and, ultimately, similar transport properties. Clearly this is not the case.

Evidence for low ion dissociation in EC/DMC can be observed directly from ^{7}Li NMR, as shown in Figure 7. Here the half-width of the lithium peak is plotted for all solutions, with an example series at 0.01 M polymer plotted in Figure 7A. The lithium peak width is significantly larger in all EC/DMC solutions with polymer but is narrow for pure LiTFSI in EC/DMC and all DMSO solutions. NMR peak broadening or narrowing can be due to a range of potential causes, but a reasonable explanation for the data shown in Figure 7 is that lithium associated with a polymer would move significantly more slowly and thus its signal would be less resolved, as is typical for polymers in NMR.[65] In addition, this trend cannot be explained by the bulk viscosity, as the 0.01 and 0.1 M polymer in EC/DMC solutions display the same trend in peak width, despite displaying significantly different trends in

viscosity. Therefore, we use the peak width here as a proxy for the relative degree of association between Li$^+$ and the polyions, with a larger peak width corresponding to a higher degree of association.

There are two possible explanations for the apparently higher ion association in EC/DMC than DMSO. First, if the polymer conformation is coiled tightly, one might expect the lithium counterions to be trapped within some form of micellar structure. Second, despite having similar dielectric constant, EC/DMC may not provide adequate solvation of the sulfonate/Li structure. To investigate this point, the dissociation constant of the polymer sulfonate group can be estimated using quantum chemistry calculations, shown in Table 1. Here

Table 1. Dissociation Constant in EC/DMC and DMSO Calculated with Implicit Solvent and Explicit Solvent

	dissociation constants	
	implicit solvent	explicit solvent
DMSO	0.59	56.40
EC/DMC	0.86	4.38

we calculate the dissociation constant of a polymer-appended ion using both an implicit solvent model and an explicit solvent model. The details of these models are described more completely in the Methods section. When solvation is approximated by an implicit solvent model, where the dielectric constant is the only parameter distinguishing DMSO and EC/DMC, we observe a lower dissociation constant (corresponding to less favorable dissociation) for DMSO. This is consistent with DMSO's slightly lower dielectric constant. With explicit solvent molecules included in the calculation, however, we see the opposite trend: dissociation is now substantially more favorable in DMSO.

This trend coincides with the differences in donor number of the solvent molecules, indicating that this may be a more essential parameter in determining ion association than the dielectric constant of the neat solvent. The utility of the donor number concept in describing dissociation of ions has been noted in polyelectrolytes before, though we note that others have suggested more advanced models that may be able to capture a wider range of behavior.[15,66] Note that the orders-of-magnitude differences in dissociation constants between the

implicit and explicit solvent calculations are due to systematic errors in solvation energy from the implicit solvent model used, which can be on the order of 0.5 eV.[67] This error is then transferred to the exponential used to calculate the dissociation constant, yielding variations consistent with the differences between methods observed in Table 1. These systematic errors, however, should not affect the observed trend between solvents.

These results suggest that conventional theories of counterion condensation in polyelectrolytes, in which the solvent is only accounted for implicitly as a dielectric continuum, do not adequately capture important trends in these systems. Although polymer conformation also likely plays a role in the observed transport properties here, neutron scattering experiments that would be necessary to probe directly the polymer radius of gyration are beyond the scope of this work. As there is a clear difference in the dissociation of lithium in the two solvents, simply from the standpoint of dissociation constant, it is reasonable to infer that the deciding factor in the poor conductivity observed in EC/DMC is the dissociation of the ion appended to the polymer backbone. In addition, though the viscosity measurement indicates a charge screening effect causing a decrease in viscosity on addition of salt, there is no evidence that the polymer is significantly charged in this solvent. The viscosity trend in EC/DMC might be explained instead by ionic interactions due to ion coordination with the ether functionality of the PEG segments[68] or strong dipolar interactions between the ion pairs that would only be present in EC/DMC. Either hypothesis requires further investigation.

Ultimately, the relative motion of lithium to the other species is the desired property, as captured by the transport number, t_+, defined in eq 5.

$$t_+ = \frac{c_{Li}D_{Li}}{c_{Li}D_{Li} + c_{TFSI}D_{TFSI} + c_{sulfonates}D_{polymer}} \quad (5)$$

Here t_+ is defined directly as the fraction of the total conductivity that would come from lithium if the Nernst–Einstein equation were valid for each species. It should be noted that this is not explicitly equivalent to the true electrochemical transference number, which would require significant electrochemical characterization that is beyond the scope of this work.[7] The transport number reported here is still a measure of the relative motion of lithium over the other species that would contribute to the conductivity. For EC/DMC in Figure 8B, t_+ of the polymer solution is high without salt, but addition of any salt immediately causes a significant drop due to the very fast-moving TFSI⁻ anion. Because a significant fraction of lithium also always diffuses slowly in this system, the t_+ of the polymer containing solutions is actually lower than that of the pure LiTFSI solution. This result is only true for the case that the polyion does not dissociate because, in contrast, the t_+ remains high even as a small molecule salt is added to the DMSO polymer solutions (Figure 8A), where substantial Li⁺–SO₃⁻ dissociation occurs. As salt concentration is increased, t_+ approaches the t_+ of the pure LiTFSI solution. This suggests in a well-dissociated solution there is the potential to optimize conductivity and t_+ by tuning small molecule salt content.

■ CONCLUSIONS

In this work, the transport properties of solutions of sulfonated polysulfone/poly(ethylene glycol) copolymer in EC/DMC and
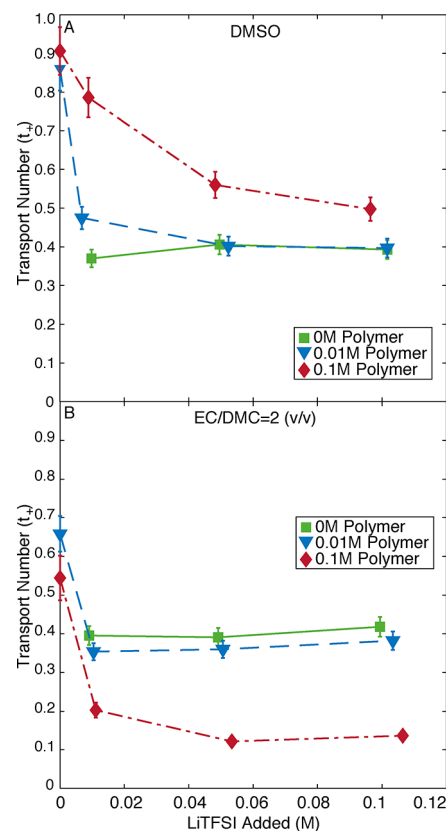
Figure 8. Transport number as a function of LiTFSI added at each polymer concentration in (A) DMSO and (B) EC/DMC = 2 (v/v).

DMSO with added LiTFSI have been investigated as a function of salt content. It is seen that the addition of salt to either solution causes an increase in solution conductivity but that the bulk viscosity only changes as a function of salt concentration at high polymer concentration in EC/DMC. The behavior of lithium in each solution is quite different, resulting in significant differences in the final transport properties. In EC/DMC, the polymer and lithium are poorly dissociated, and adding salt does not alter the properties of the solution to significantly change lithium–polymer dissociation. Thus, the conductivity of the solution with added salt is entirely due to the added salt, and changes in viscosity must be a result of another interaction, either between ether repeat units and LiTFSI or between the strong dipoles of ion pairs. In DMSO, the polymer and lithium are well-dissociated, and addition of salt causes t_+ to decrease and the conductivity not to increase as significantly as in EC/DMC. Both NMR and quantum chemistry calculations demonstrate that EC/DMC is unable to dissociate the sulfonate group on the polymer as strongly as DMSO. This alone predicts the majority of behavior observed here, suggesting the design of new HTNE polyelectrolyte solutions should strongly consider the ability of the solvent to dissociate the polyion and counterion. In the design of an HTNE for battery applications, a relatively narrow range of solvents are well-characterized, and thus structural changes to the polyion that promote dissociation are the most promising path forward. Addition of salt is shown here as a promising method to tune conductivity and transference number in the case that the polymer is well dissociated, an important ability that is not possible in most electrolytes.

■ ASSOCIATED CONTENT

Ⓢ Supporting Information

The Supporting Information is available free of charge on the ACS Publications website at DOI: 10.1021/acs.macromol.8b01696.

Example PFG-NMR data and solvent diffusion coefficients plotted individually (PDF)

■ AUTHOR INFORMATION

Corresponding Author

*E-mail bmcclosk@berkeley.edu.

ORCID Ⓞ

Kyle M. Diederichsen: 0000-0002-6787-7996

Kara D. Fong: 0000-0002-0711-097X

Kristin A. Persson: 0000-0003-2495-5509

Bryan D. McCloskey: 0000-0001-6599-2336

Notes

The authors declare no competing financial interest.

■ ACKNOWLEDGMENTS

■ REFERENCES

(1) Doyle, M.; Fuller, T. F.; Newman, J. The Importance of the Lithium Ion Transference Number in Lithium/Polymer Cells. *Electrochim. Acta* **1994**, *39*, 2073−2081.

(2) Diederichsen, K. M.; McShane, E. J.; McCloskey, B. D. Promising Routes to a High Li⁺ Transference Number Electrolyte for Lithium Ion Batteries. *ACS Energy Lett.* **2017**, *2*, 2563−2575.

(3) Xu, K.; Lam, Y.; Zhang, S. S.; Jow, T. R.; Curtis, T. B. Solvation Sheath of Li⁺ in Nonaqueous Electrolytes and Its Implication of Graphite/Electrolyte Interface Chemistry. *J. Phys. Chem. C* **2007**, *111*, 7411−7421.

(4) Goodenough, J. B.; Kim, Y. Challenges for Rechargeable Li Batteries. *Chem. Mater.* **2010**, *22*, 587−603.

(5) Winter, M.; Besenhard, J. O. J.; Spahr, M. E.; Novák, P. Insertion Electrode Materials for Rechargeable Lithium Batteries. *Adv. Mater.* **1998**, *10*, 725−763.

(6) Flamme, B.; Rodriguez Garcia, G.; Weil, M.; Haddad, M.; Phansavath, P.; Ratovelomanana-Vidal, V.; Chagnes, A. Guidelines to Design Organic Electrolytes for Lithium-Ion Batteries: Environmental Impact, Physicochemical and Electrochemical Properties. *Green Chem.* **2017**, *19*, 1828−1849.

(7) Valøen, L. O.; Reimers, J. N. Transport Properties of LiPF₆-Based Li-Ion Battery Electrolytes. *J. Electrochem. Soc.* **2005**, *152*, A882.

(8) Kerman, K.; Luntz, A.; Viswanathan, V.; Chiang, Y.-M.; Chen, Z. Review—Practical Challenges Hindering the Development of Solid State Li-Ion Batteries. *J. Electrochem. Soc.* **2017**, *164*, A1731−A1744.

(9) Zhang, H.; Li, C.; Piszcz, M.; Coya, E.; Rojo, T.; Rodriguez-Martinez, L. M.; Armand, M. B.; Zhou, Z. Single Lithium-Ion Conducting Solid Polymer Electrolytes: Advances and Perspectives. *Chem. Soc. Rev.* **2017**, *46*, 797−815.

(10) Cheng, X.; Pan, J.; Zhao, Y.; Liao, M.; Peng, H. Gel Polymer Electrolytes for Electrochemical Energy Storage. *Adv. Energy Mater.* **2018**, *8*, 1702184.

(11) Tu, Z.; Choudhury, S.; Zachman, M. J.; Wei, S.; Zhang, K.; Kourkoutis, L. F.; Archer, L. A. Designing Artificial Solid-Electrolyte Interphases for Single-Ion and High-Efficiency Transport in Batteries. *Joule* **2017**, *1*, 394.

(12) Zhao, C.-Z.; Zhang, X.-Q.; Cheng, X.-B.; Zhang, R.; Xu, R.; Chen, P.-Y.; Peng, H.-J.; Huang, J.-Q.; Zhang, Q. An Anion-Immobilized Composite Electrolyte for Dendrite-Free Lithium Metal Anodes. *Proc. Natl. Acad. Sci. U. S. A.* **2017**, *114*, 11069−11074.

(13) Kreuer, K.-D.; Wohlfarth, A.; de Araujo, C. C.; Fuchs, A.; Maier, J. Single Alkaline-Ion (Li⁺, Na⁺) Conductors by Ion Exchange of Proton-Conducting Ionomers and Polyelectrolytes. *ChemPhysChem* **2011**, *12*, 2558−2560.

(14) Buss, H. G.; Chan, S. Y.; Lynd, N. A.; McCloskey, B. D. Nonaqueous Polyelectrolyte Solutions as Liquid Electrolytes with High Lithium Ion Transference Number and Conductivity. *ACS Energy Lett.* **2017**, *2*, 481−487.

(15) Smiatek, J.; Wohlfarth, A.; Holm, C. The Solvation and Ion Condensation Properties for Sulfonated Polyelectrolytes in Different Solvents—a Computational Study. *New J. Phys.* **2014**, *16*, 025001.

(16) Xu, K. Nonaqueous Liquid Electrolytes for Lithium-Based Rechargeable Batteries. *Chem. Rev.* **2004**, *104*, 4303−4418.

(17) Muthukumar, M. 50th Anniversary Perspective : A Perspective on Polyelectrolyte Solutions. *Macromolecules* **2017**, *50*, 9528−9560.

(18) Mitsuru Nagasawa Aaron, R.; Dinner, S. A. R. *Physical Chemistry of Polyelectrolyte Solutions*; 2015; Vol. *158*.

(19) *Physical Chemistry of Polyelectrolytes*; Radeva, T., Ed.; 2001.

(20) Dobrynin, A. V. *Solutions of Charged Polymers*; Elsevier B.V.: 2012; Vol. *1*.

(21) Hara, M. Polyelectrolytes in Nonaqueous Solutions. In *Physical Chemistry of Polyelectrolytes*; Radeva, T., Ed.; 2001; pp 245−279.

(22) Hara, M. Polyelectrolytes in Nonaqueous Solution. In *Polyelectrolytes Science and Technology*; Hara, M., Ed.; Marcel Dekker: 1993; pp 193−264.

(23) Bordi, F.; Cametti, C.; Colby, R. H. Dielectric Spectroscopy and Conductivity of Polyelectrolyte Solutions. *J. Phys.: Condens. Matter* **2004**, *16*, R1423−R1463.

(24) Prabhu, V. M. Counterion Structure and Dynamics in Polyelectrolyte Solutions. *Curr. Opin. Colloid Interface Sci.* **2005**, *10*, 2−8.

(25) Dobrynin, A. V.; Rubinstein, M. Counterion Condensation and Phase Separation in Solutions of Hydrophobic Polyelectrolytes. *Macromolecules* **2001**, *34*, 1964−1972.

(26) Manning, G. S. Limiting Laws and Counterion Condensation in Polyelectrolyte Solutions. III. An Analysis Based on the Mayer Ionic Solution Theory. *J. Chem. Phys.* **1969**, *51*, 3249−3252.

(27) Manning, G. S. Limiting Laws and Counterion Condensation in Polyelectrolyte Solutions II. Self-Diffusion of the Small Ions. *J. Chem. Phys.* **1969**, *51*, 934−938.

(28) Manning, G. S. Limiting Laws and Counterion Condensation in Polyelectrolyte Solutions I. Colligative Properties. *J. Chem. Phys.* **1969**, *51*, 924−933.

(29) Dobrynin, A. V.; Colby, R. H.; Rubinstein, M. Scaling Theory of Polyelectrolyte Solutions. *Macromolecules* **1995**, *28*, 1859−1871.

(30) De Gennes, P. G.; Pincus, P.; Velasco, R. M.; Brochard, F. Remarks on Polyelectrolyte Conformation. *J. Phys. (Paris)* **1976**, *37*, 1461−1473.

(31) Muthukumar, M. Theory of Counter-Ion Condensation on Flexible Polyelectrolytes: Adsorption Mechanism. *J. Chem. Phys.* **2004**, *120*, 9343−9350.

(32) Diederichsen, K. M.; Buss, H. G.; McCloskey, B. D. The Compensation Effect in the Vogel−Tammann−Fulcher (VTF) Equation for Polymer-Based Electrolytes. *Macromolecules* **2017**, *50*, 3831−3840.

(33) Wandrey, C.; Hunkeler, D.; Wendler, U.; Jaeger, W. Counterion Activity of Highly Charged Strong Polyelectrolytes. *Macromolecules* **2000**, *33*, 7136−7143.

(34) Hara, M.; Wu, J.; Lee, A. H. Solution Properties of Ionomers. 2. Simple Salt Effect. *Macromolecules* **1989**, *22*, 754−757.

(35) Holz, M.; Weingartner, H. Calibration in Accurate Spin-Echo Self-Diffusion Measurements Using 1H and Less-Common Nuclei. *J. Magn. Reson.* **1991**, *92*, 115−125.

(36) Holz, M.; Mao, X.; Seiferling, D.; Sacco, A. Experimental Study of Dynamic Isotope Effects in Molecular Liquids: Detection of Translation-rotation Coupling. *J. Chem. Phys.* **1996**, *104*, 669−679.

(37) Hayamizu, K.; Aihara, Y.; Arai, S.; Martinez, C. G. Pulse-Gradient Spin-Echo 1H, 7Li, and 19F NMR Diffusion and Ionic Conductivity Measurements of 14 Organic Electrolytes Containing LiN(SO$_2$CF$_3$)$_2$. *J. Phys. Chem. B* **1999**, *103*, 519−524.

(38) Jerschow, A.; Müller, N. Suppression of Convection Artifacts in Stimulated-Echo Diffusion Experiments. Double-Stimulated-Echo Experiments. *J. Magn. Reson.* **1997**, *125*, 372−375.

(39) Wu, D. H.; Chen, A. D.; Johnson, C. S. An Improved Diffusion-Ordered Spectroscopy Experiment Incorporating Bipolar-Gradient Pulses. *J. Magn. Reson., Ser. A* **1995**, *115*, 260−264.

(40) Sinnaeve, D. The Stejskal-Tanner Equation Generalized for Any Gradient Shape-an Overview of Most Pulse Sequences Measuring Free Diffusion. *Concepts Magn. Reson., Part A* **2012**, *40A*, 39−65.

(41) *Gaussian 16*, Revision B.01: Frisch, M. J.; Trucks, G. W.; Schlegel, H. B.; Scuseria, G. E.; Robb, M. A.; Cheeseman, J. R.; Scalmani, G.; Barone, V.; Petersson, G. A.; Nakatsuji, H.; Li, X.; Caricato, M.; Marenich, A. V.; Bloino, J.; Janesko, B. G.; Gomper, D. J. Gaussian, Inc.: Wallingford, CT, 2016.

(42) Chai, J.-D.; Head-Gordon, M. Long-Range Corrected Hybrid Density Functionals with Damped Atom−Atom Dispersion Corrections. *Phys. Chem. Chem. Phys.* **2008**, *10*, 6615.

(43) Krishnan, R.; Binkley, J. S.; Seeger, R.; Pople, J. A. Self-Consistent Molecular Orbital Methods. XX. A Basis Set for Correlated Wave Functions. *J. Chem. Phys.* **1980**, *72*, 650−654.

(44) Clark, T.; Chandrasekhar, J.; Spitznagel, G. W.; Schleyer, P. V. R. Efficient Diffuse Function-augmented Basis Sets for Anion Calculations. III. The 3-21+G Basis Set for First-row Elements. *J. Comput. Chem.* **1983**, *4*, 294−301.

(45) McLean, A. D.; Chandler, G. S. Contracted Gaussian Basis Sets for Molecular Calculations. I. Second Row Atoms, Z = 11−18. *J. Chem. Phys.* **1980**, *72*, 5639−5648.

(46) Tomasi, J.; Mennucci, B.; Cancès, E. The IEF Version of the PCM Solvation Method: An Overview of a New Method Addressed to Study Molecular Solutes at the QM Ab Initio Level. *J. Mol. Struct.: THEOCHEM* **1999**, *464*, 211−226.

(47) Mennucci, B.; Cancès, E.; Tomasi, J. Evaluation of Solvent Effects in Isotropic and Anisotropic Dielectrics and in Ionic Solutions with a Unified Integral Equation Method: Theoretical Bases, Computational Implementation, and Numerical Applications. *J. Phys. Chem. B* **1997**, *101*, 10506−10517.

(48) Mennucci, B.; Tomasi, J. Continuum Solvation Models: A New Approach to the Problem of Solute's Charge Distribution and Cavity Boundaries. *J. Chem. Phys.* **1997**, *106*, 5151−5158.

(49) Cancès, E.; Mennucci, B.; Tomasi, J. A New Integral Equation Formalism for the Polarizable Continuum Model: Theoretical Background and Applications to Isotropic and Anisotropic Dielectrics. *J. Chem. Phys.* **1997**, *107*, 3032−3041.

(50) MacGregor, W. S. The Chemical and Physical Properties of DMSO. *Ann. N. Y. Acad. Sci.* **1967**, *141*, 3−12.

(51) Naejus, R.; Lemordant, D.; Coudert, R.; Willmann, P. Excess Thermodynamic Properties of Binary Mixtures Containing Linear or Cyclic Carbonates as Solvents at the Temperatures 298.15 and 315.15 K. *J. Chem. Thermodyn.* **1997**, *29*, 1503−1515.

(52) Self, J.; Wood, B. M.; Rajput, N. N.; Persson, K. A. The Interplay between Salt Association and the Dielectric Properties of Low Permittivity Electrolytes: The Case of LiPF$_6$ and LiAsF$_6$ in Dimethyl Carbonate. *J. Phys. Chem. C* **2018**, *122*, 1990−1994.

(53) Onthong, U.; Megyes, T.; Bakó, I.; Radnai, T.; Hermansson, K.; Probst, M. Molecular Dynamics Simulation of Lithium Iodide in Liquid Dimethylsulfoxide. *Chem. Phys. Lett.* **2005**, *401*, 217−222.

(54) Megyes, T.; Bakó, I.; Radnai, T.; Grósz, T.; Kosztolányi, T.; Mroz, B.; Probst, M. Structural Investigation of Lithium Iodide in Liquid Dimethyl Sulfoxide: Comparison between Experiment and Computation. *Chem. Phys.* **2006**, *321*, 100−110.

(55) Borodin, O.; Smith, G. D. Quantum Chemistry and Molecular Dynamics Simulation Study of Dimethyl Carbonate: Ethylene Carbonate Electrolytes Doped with LiPF$_6$. *J. Phys. Chem. B* **2009**, *113*, 1763−1776.

(56) *MacroModel*; Schrödinger, LLC: New York, 2018.

(57) Gering, K. L. Prediction of Electrolyte Conductivity: Results from a Generalized Molecular Model Based on Ion Solvation and a Chemical Physics Framework. *Electrochim. Acta* **2017**, *225*, 175−189.

(58) Jia, P.; Yang, Q.; Gong, Y.; Zhao, J. Dynamic Exchange of Counterions of Polystyrene Sulfonate. *J. Chem. Phys.* **2012**, *136*, 084904.

(59) Bordi, F.; Cametti, C.; Gili, T. Electrical Conductivity of Polyelectrolyte Solutions in the Presence of Added Salt: The Role of the Solvent Quality Factor in Light of a Scaling Approach. *Phys. Rev. E: Stat. Phys., Plasmas, Fluids, Relat. Interdiscip. Top.* **2003**, *68*, 011805.

(60) Vink, H. Investigation of Local Viscosity in Polymer Solutions by Means of Electrolytic Conductivity. *Polymer* **1982**, *23*, 6−9.

(61) Timachova, K.; Chintapalli, M.; Olson, K. R.; Mecham, S. J.; DeSimone, J. M.; Balsara, N. P. Mechanism of Ion Transport in Perfluoropolyether Electrolytes with a Lithium Salt. *Soft Matter* **2017**, *13*, 5389−5396.

(62) Krachkovskiy, S. A.; Bazak, J. D.; Fraser, S.; Halalay, I. C.; Goward, G. R. Determination of Mass Transfer Parameters and Ionic Association of LiPF$_6$: Organic Carbonates Solutions. *J. Electrochem. Soc.* **2017**, *164*, A912−A916.

(63) Muthukumar, M. Dynamics of Polyelectrolyte Solutions. *J. Chem. Phys.* **1997**, *107*, 2619−2635.

(64) Hall, D. S.; Self, J.; Dahn, J. R. Dielectric Constants for Quantum Chemistry and Li-Ion Batteries: Solvent Blends of Ethylene Carbonate and Ethyl Methyl Carbonate. *J. Phys. Chem. C* **2015**, *119*, 22322−22330.

(65) Abbrent, S.; Greenbaum, S. Recent Progress in NMR Spectroscopy of Polymer Electrolytes for Lithium Batteries. *Curr. Opin. Colloid Interface Sci.* **2013**, *18*, 228−244.

(66) Nakamura, I.; Shi, A. C.; Wang, Z. G. Ion Solvation in Liquid Mixtures: Effects of Solvent Reorganization. *Phys. Rev. Lett.* **2012**, *109*, 1−5.

(67) Pliego, J. R.; Riveros, J. M. The Cluster−Continuum Model for the Calculation of the Solvation Free Energy of Ionic Species. *J. Phys. Chem. A* **2001**, *105*, 7241−7247.

(68) Lundberg, R. D.; Bailey, F. E.; Callard, R. W. Interactions of Inorganic Salts with Poly(Ethylene Oxide). *J. Polym. Sci., Part A-1: Polym. Chem.* **1966**, *4*, 1563−1577.